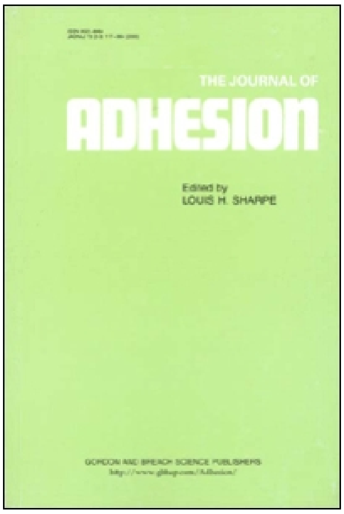

The Journal of Adhesion
Publication details, including instructions for authors and subscription information:
http://www.informaworld.com/smpp/title~content=t713453635

THE EFFECT OF COMPOSITION ON SURFACE PROPERTIES OF POLYESTER-MELAMINE THERMOSET COATINGS

Christopher A. Lukey[a]; Hugh R. Brown[a]; Geoffrey M. Spinks[a]; David P. Buxton[b]
[a] Steel Institute, University of Wollongong, Wollongong, NSW, Australia [b] Blue Scope Steel Research, Port Kembla, NSW, Australia

To cite this Article Lukey, Christopher A. , Brown, Hugh R. , Spinks, Geoffrey M. and Buxton, David P.(2004) 'THE EFFECT OF COMPOSITION ON SURFACE PROPERTIES OF POLYESTER-MELAMINE THERMOSET COATINGS', The Journal of Adhesion, 80: 7, 647 — 660

To link to this Article: DOI: 10.1080/00218460490477134

URL: http://dx.doi.org/10.1080/00218460490477134

The Journal of Adhesion, 80: 647–660, 2004

ISSN: 0021-8464 print/1545-5823 online
DOI: 10.1080/00218460490477134

THE EFFECT OF COMPOSITION ON SURFACE PROPERTIES OF POLYESTER–MELAMINE THERMOSET COATINGS

Christopher A. Lukey
Hugh R. Brown
Geoffrey M. Spinks
Steel Institute, University of Wollongong, Wollongong,
NSW, Australia

David P. Buxton
Blue Scope Steel Research, Port Kembla, NSW, Australia

Surface properties of polyester-melamine thermoset coatings have been investigated using XPS, thermal analysis methods, surface energy measurement, and small particle adhesion using a dedicated force rig. Bulk glass transition temperatures and surface energies changed little over a wide composition range (5–50 wt% melamine). At low melamine content (<20 wt%), particle adhesion behaviour was similar to that of pressure-sensitive adhesives; however, at high melamine contents particle adhesion was uniformly negligible. XPS and thermal analysis showed that at high melamine concentrations the surface melamine content was higher than expected, suggesting the formation of a hard, highly crosslinked, self-condensed, melamine-rich surface layer. This was not observed at lower melamine concentrations. The presence of this glassy melamine-rich surface layer is believed to be responsible for the low particle adhesion at high melamine concentrations.

Keywords: Polyester-melamines; Coatings; Surface energy; XPS; Particle adhesion

INTRODUCTION

In two-component crosslinking thermoset systems such as epoxy-amines, polyester-melamines, etc., the most obvious way to modify

Received 20 January 2004; in final form 16 April 2004.

We thank the Australian Research Council, BlueScope Steel Ltd., and the University of Wollongong for funding this work. We also thank BlueScope Steel Research for providing materials and access to analytical instrumentation, including XPS.

Address correspondence to Christopher A. Lukey, Steel Institute, University of Wollongong, Wollongong, NSW 2522, Australia. E-mail: chris_lukey@uow.edu.au

the properties of the final product is to vary the relative concentrations of the base resin and the crosslinker. Assuming the components are well mixed and the resultant crosslinked polymer structure is homogeneous, one might expect the properties to range from base−resin-like at low crosslinker concentrations, through an "optimum" at a certain crosslinker concentration (which may or may not be related to the chemical reaction stoichiometry), to crosslinker-like at high crosslinker concentrations. In practice, however, the structures of such systems are commonly not homogeneous, and the properties depend more on reactant miscibility and molecular mobility considerations, as well as chemical reactions other than simple condensation between resin and crosslinker. In a recent series of publications by Gamage *et al.* [1, 2], for example, it was shown that for a saturated, isophthalate-containing hydroxy-functional polyester crosslinked with hexamethoxymethylmelamine (HMMM) and cured under nonisothermal conditions there exists a threshold concentration of HMMM, above which phase-separated structures similar to interpenetrating networks (IPNs) are generated, and HMMM appears to preferentially self-condense at the air-coating interface. Thus, a major change in surface properties might be expected in this system as the HMMM concentration is increased. It should be noted, however, that in related systems cured isothermally, no such phase-separated IPN-like structures have been reported.

Small particle adhesion to polymers is of both theoretical and practical interest. Modern theoretical interest stems from a desire to describe the particle adhesion and removal processes in terms of fracture mechanics and to compare particle adhesion processes with those of other adhesion phenomena. The classical description of adhesion, pioneered by Dupré in 1869 [3], is in terms of the equilibrium work of adhesion (W_A), which is described as the free energy change when the particle is brought into contact with the surface. The fracture energy, G_C, as described by Kendall [4], measured in a separation process, is always greater than W_A due to contributions other than changes in surface and interfacial energy. The difference between G_C and W_A is, however, very material dependent. For example, recently it was shown [5] that G_C for removal of a micron-scale glass particle from an elastomer surface was more than an order of magnitude greater than W_A.

Practical interest in particle adhesion is driven to a large extent by a desire to reduce adhesion between particles and polymer surfaces. Reduced adhesion finds applications in such areas as the development of contamination-resistant building facades.

In the study reported here, the effect of composition on both bulk and surface properties for a series of polyester-melamine surface coatings with a range of melamine concentrations was investigated. In particular, we describe the adhesion behaviour between a micron-scale zirconia sphere and the polyester-melamine surface as a function of composition and temperature. The instrument used was a dedicated force sensor rig that was described previously [6].

EXPERIMENTAL

Materials

The hydroxy-functional polyester used throughout this investigation consisted of a 6:4 mole ratio mixture of isophthalic acid and adipic acid, copolymerised with a 9:1 mixture of neopentyl glycol and trimethylol propane. The ratio of acid to hydroxy functionality was adjusted in order to produce a hydroxy-functional polyester of average molecular weight (M_W) 2500 and functionality ~3 hydroxy groups per molecule. The polyester was dissolved in ethyl ethoxypropionate at a concentration of 60 wt%.

Crosslinked coatings were formulated by varying the composition from 95:5 to 50:50 polyester/hexamethoxymethylmelamine (HMMM, Cyanamid Cymel 303, Cytek, W. Paterson, NJ, USA) crosslinker, on a mass percentage basis. Blocked acid catalyst, isopropylamine dodecyl benzene sulfonic acid (Cyanamid Cycat 600) was added at 2 wt% with respect to HMMM, and a small amount (0.2 wt%) of a polyether silicone surfactant (Byk Chemie BYK 306, BYK Chemie, Wesel, Germany) was added to improve film-forming ability. The viscosity of the liquid formulation was then adjusted by the addition of a hydrocarbon solvent (Exxon Solvesso 150) prior to coating.

The formulations were coated onto aluminium panels using a #32 stainless steel drawdown bar, then baked in a ventilated air oven at 300°C until the metal substrate reached a temperature of 245°C (referred to as the *Peak Metal Temperature*, or PMT), quenched in water and air dried. For DSC measurements, the samples were coated onto silicone release-coated aluminium panels and cured in the same way. The nominal dry film thickness for all formulations was 20 μm.

Adhesion Force Measurement

The adhesion force between the coating surface and a spherical, 26 μm diameter zirconia particle was determined as a function of temperature in dry nitrogen atmosphere, using a custom-built force rig as described by Toikka *et al.* [6]. The apparatus, based upon atomic force microscopy (AFM), was constructed so that a single contact could be made between a particle attached to an AFM cantilever and the sample surface for a known time before removal and measurement of the pull-off force. Briefly, using polymethyl methacrylate (PMMA) a zirconia sphere is glued to a high spring constant (typically 40 N/m) AFM imaging cantilever, which is clamped to a displacement arm attached to a precision rail. The vertical position of the displacement arm is governed by a piezoelectric crystal-controlled inchworm (Burleigh, Fishers, NY, USA). This system allows the zirconia sphere to be held at a particular vertical position for extended time periods without significant creep. Cantilever deflection is detected by reflecting the output of a focusable solid-state laser (Edmund Scientific, 1mW, $\lambda = 670\,\text{nm}$, Edmund Scientific, Barrington, NJ, USA) from the back of the cantilever onto a 4-segment position-sensing device, similar to the detector systems of many commercial AFM instruments. Thus, a change in cantilever deflection is recorded as a detector voltage change. The sample is placed on a heated stage that allows the temperature to be set between 20 and 70°C. The displacement arm, cantilever, and sample stage are located inside an environmental chamber that is purged with dry nitrogen throughout the experiment. For more detail on the construction of the device, the reader is referred to Toikka *et al.* [6]. A "typical" pull-off event is shown in Figure 1.

The conversion between detector voltage change and force is given by Equation (1):

$$F_p = \frac{k\Delta V}{Cr}, \tag{1}$$

where F_p is the pull-off force, divided by particle radius; ΔV is the detector voltage change during pull-off; k is the cantilever spring constant; C is the compliance factor (see text); and r is the particle diameter.

The compliance factor, C, provides the conversion between detector voltage and cantilever displacement. C is obtained by measuring the slope obtained when the pull-off experiment is conducted using a flat, noncompliant, nonadhering surface such as aluminium or silicon. Displacement is then converted to force using the cantilever spring constant, k.

Previous studies (T. T. Tran, H. K. Brown, and G. M. Spinks, unpublished results) of particle adhesion to a related system showed that particle adhesion increased with contact time up to 30 min, where a plateau adhesion value was reached, so in the present work this contact time was employed. The reported pull-off forces are the average of 3 contacts in different locations on the sample, with

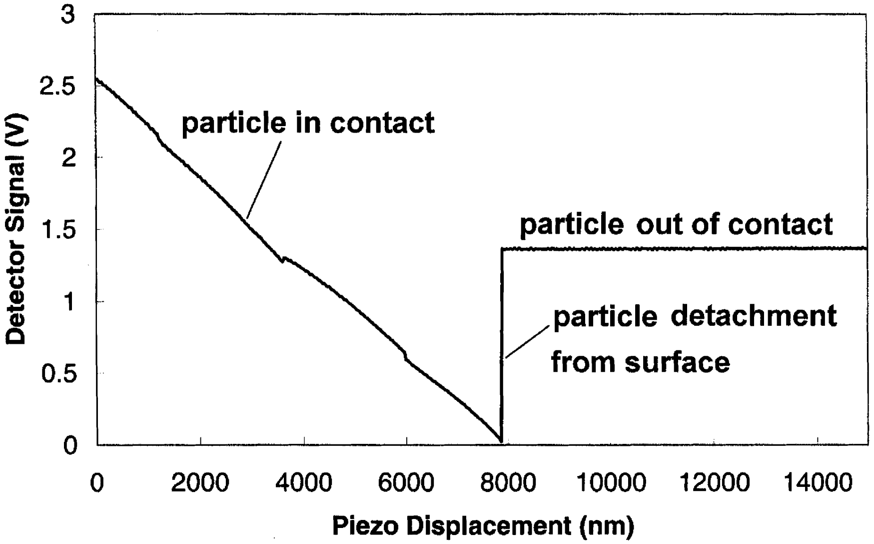

FIGURE 1 Typical force sensor output.

UV-ozone cleaning of the particle between contacts. The pull-off force was measured at decade temperature intervals from 20 to 70°C. In general, the pull-off force measurements for a particular sample at a given temperature agreed to within ±10%. Zirconia was chosen because spherical particles can be prepared with surfaces that are extremely smooth on a microscopic scale, thereby reducing the scatter in the adhesion data [6].

Note that according to the theory of contact mechanics developed by Johnson *et al.* [4, 7], the applied load does not impact on the pull-off force. The adhesion force apparatus used in this work is not able to measure the applied load, and it is, therefore, probable that every contact experiment involves a *different* applied load. The reproducibility of the pull-off force measurements, however, is good, suggesting that the applied load is unimportant, consistent with the contact mechanics theory developed by Johnson, Kendall, and Roberts [7].

Glass Transition Temperature Measurement

Two measures of the glass transition temperature were used: thermomechanical analysis (TMA) and differential scanning calorimetry (DSC). The onset of bulk softening was obtained using a Perkin Elmer TMA7 Thermomechanical Analyser (Perkin Elemer, Boston, MA, USA) in penetration probe mode. Samples were heated in a N_2

atmosphere from −10°C to 60°C at 20°C/min and analysed using a 1 mm diameter hemispherical quartz probe with a probe force of 50 mN. DSC measurements were obtained using a TA Instruments Q100 Differential Scanning Calorimeter (TA Instruments, New Castle, DE, USA). Samples were heated in a nitrogen atmosphere from −10°C to 60°C at 20°C/min, and Tg was taken as the inflection point of the change in heat flow.

Surface Energy Measurement

Surface energies were calculated from two-liquid equilibrium contact angle measurements, using a Ramé Hart Model 100-00 NRL Contact Angle Goniometer (Ramé Hart, Mt. Lakes, NJ, USA). Contact angles for water and di-iodomethane were measured at room temperature, from which the polar ($\gamma_s{}^p$) and dispersive ($\gamma_s{}^d$) components of the surface energies were calculated using the Geometric Mean relationship [8, 9]. The total surface energy was then the sum of $\gamma_s{}^p$ and $\gamma_s{}^d$.

Surface Elemental Composition

X-ray photoelectron spectroscopy (XPS) was used to determine the surface elemental composition, for comparison with the theoretical bulk composition. The instrument used was a VG Scientific ESCALAB 220i-XL (VG Scientific, Hastings, UK). The silicone surfactant, used to improve film-forming ability, was removed from the surface prior to XPS analysis by washing with a 1:1 mixture of ethanol and isopropyl alcohol with ultrasonic agitation for 1 h.

For deconvolution of C_{ls} spectra, curve fitting was performed using binding energies, peak widths, and shapes reported in recent literature [10−12]. Table 1 shows the band parameters used for the deconvolution. Note that the C−O band at 286.8 eV was not used in

TABLE 1 Band Positions for Deconvolution of C_{ls} XPS Spectra

Band	Binding energy (eV)
Aromatic C−H*	284.3
Aliphatic C−H*	285.0
C−O*	286.8
C−N	287.8
C = O	288.9

*Not used in further calculations (see text).

further data analysis, as this band can arise from polyester, melamine, and the crosslinked polymer. It was, however, included in the calculation of total carbon. Likewise, the bands at 284.3 eV (aromatic C–H) and 285.0 eV (aliphatic C–H) were not used for analysis due to the number of sources, but were included in total carbon. The full width at half maximum of all the deconvoluted bands was constrained within the range 1.65–1.85 eV, and the Gaussian–Lorentzian mixture was kept constant, enabling all spectra to be fitted satisfactorily. Goodness of fit was assessed by area of residuals, and any fitting with area residuals greater than 3% of total area was discarded. The binding energy scale was corrected according to common convention [11] to the aliphatic C-H band at 285.00 eV.

RESULTS AND DISCUSSION

The pull-off force for a zirconia particle in contact with the coating surface was measured at decade temperature intervals for crosslinked polyester film samples of various HMMM concentrations. The results show a profound effect of HMMM content on the pull-off force, especially at low temperatures (<50°C), as shown in Figure 2. Samples with 5 and 10 wt% HMMM showed high adhesion at 30°C, whereas samples with HMMM content 20 wt% and above showed very low adhesion, irrespective of temperature. At higher temperatures, all formulations showed similar low adhesion.

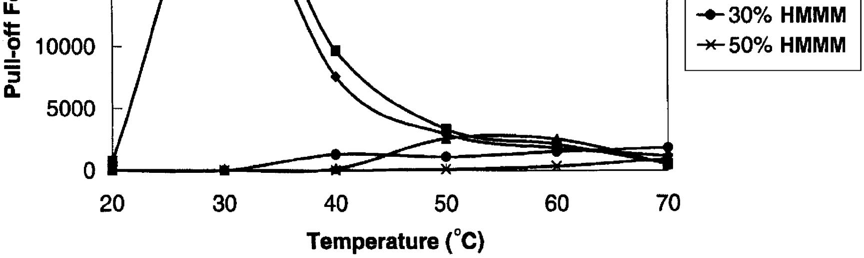

FIGURE 2 Pull-off force as a function of temperature for HMMM/polyesters with varying HMMM concentration.

Toikka *et al.* [6] recently described the adhesion behaviour of zirconia particles and a commercial polyester-melamine paint resin of unknown melamine content, and found that adhesion was very low (~300 mN/m) at temperatures below the bulk Tg, and that it reached a maximum (~12000 mN/m) slightly above Tg before declining again as the temperature was further increased. They compared the measured pull-off force with a theoretical pull-off force of 966 mN/m, calculated on the assumption that detachment involves only changes in surface/interfacial energy. The lower-than-expected pull-off force below Tg was explained in terms of reduced contact due to surface asperities, leading to a reduced contribution from the dominant van der Waals interaction. Above Tg, the very large increase in adhesion was likened to the behaviour of pressure-sensitive adhesives. The higher adhesion for such materials is thought to be associated with the balance between adhesion energy and viscoelastic energy loss as the surface becomes increasingly rubbery. The adhesion maximum occurs when the ability to make intimate contact and the ability to store and dissipate energy are optimised during detachment. This mechanism also explains the large decrease in pull-off force as the temperature is further increased, since energy dissipation is greatly reduced.

The glass transition temperature as a function of HMMM content is shown in Figure 3, measured using TMA and DSC. DSC measures Tg as a change in heat flow associated with free volume change, whereas TMA measures the onset of bulk softening, so the two values would be expected to be slightly different, as seen in the figure. TMA values varied over a roughly 10°C range as a function of HMMM content with a maximum at 10 wt% HMMM. DSC gave a greater range of Tg values (6−23°C), but the trends were the same as for TMA. These results are consistent with the results of a previous study [1] where Tgs of detached films were measured using DSC. DSC data show that all compositions except for 10 wt% HMMM gave coatings with Tg < 20°C, the minimum temperature attainable using the adhesion force apparatus. Thus, all samples except for 10 wt% HMMM were in the rubbery state at the minimum temperature used.

Comparing the adhesion data in Figure 2 with the Tg (DSC) results shown in Figure 3, some significant differences can be seen. It appears that at low HMMM contents (10 wt% or less), the behaviour is similar to that of pressure-sensitive adhesives, as described previously. That is, a distinct adhesion maximum occurred at a temperature slightly above the bulk Tg before a significant decrease in adhesion as the temperature was further increased. This behaviour is thus similar to that described previously [6] and explained in terms of the behaviour

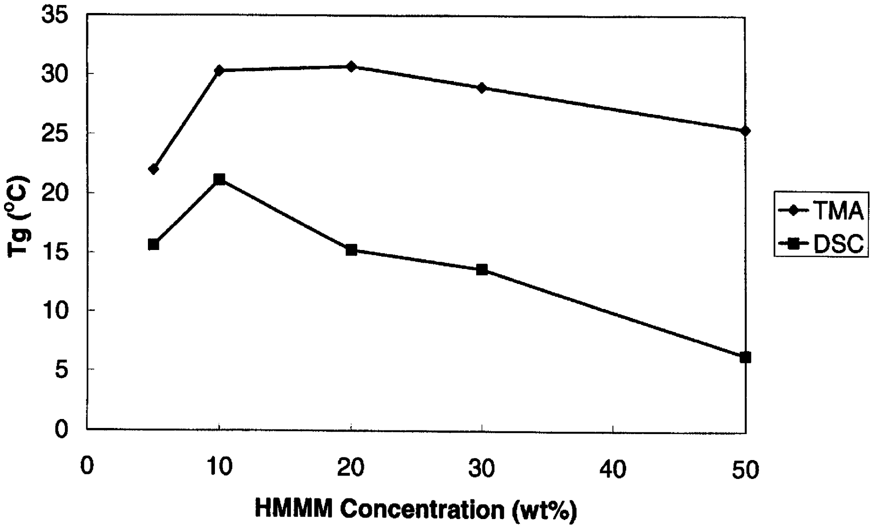

FIGURE 3 Tg measurements (TMA and DSC) for HMMM/polyesters, as a function of HMMM concentration.

of pressure-sensitive adhesives. However, very different behaviour was observed for higher HMMM contents (20 wt% or more). In such cases, the adhesion maxima were not distinct and tended to occur at temperatures well in excess of the bulk Tg. Clearly factors other than the bulk Tg must also affect particle adhesion.

Equilibrium solid-surface energy ($\gamma_s{}^p$, $\gamma_s{}^d$, and $\gamma_s{}^t$) as a function of HMMM concentration are shown in Figure 4. Although there is some scatter in the data, within experimental error no obvious trend in surface energy can be discerned for the different crosslinker concentrations used. Thus, surface energy considerations cannot explain the particle adhesion behaviour described above.

Relevant data from XPS analysis are shown in Figure 5. The figure shows, as expected, an increase in the surface nitrogen concentration as the HMMM content increased, with a concomitant decrease in carbon and oxygen. According to a recent publication [2], two measures of surface composition can be derived from XPS measurements. The ratio of total N/total C in the surface gives a good first approximation of the amount of melamine-containing species in the surface, since melamine is the only source of nitrogen in the formulation. Carbon, however, derives from both melamine and polyester. Figure 6 compares experimental N/C with the calculated ratio based upon both no reaction (NR, *i.e.*, physical mixture of the two

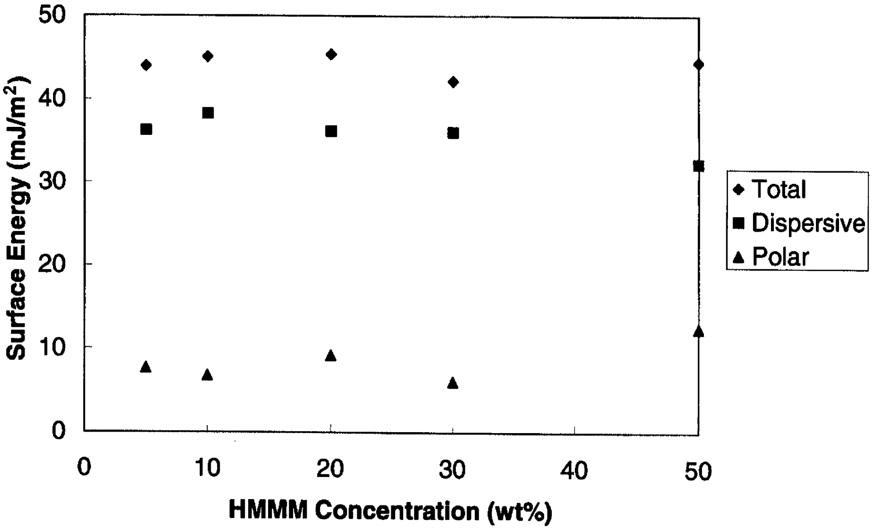

FIGURE 4 Equilibrium solid surface energy for HMMM/polyesters, as a function of HMMM concentration.

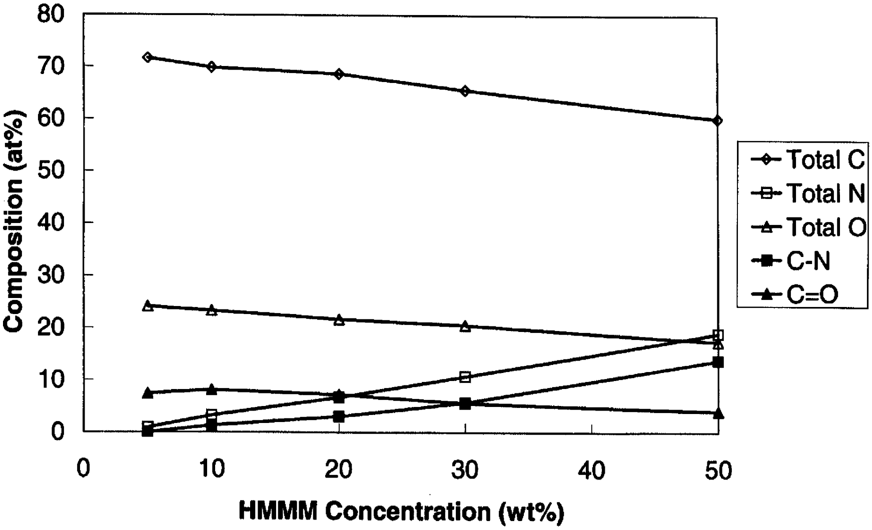

FIGURE 5 Surface composition of HMMM/polyesters, as a function of HMMM concentration.

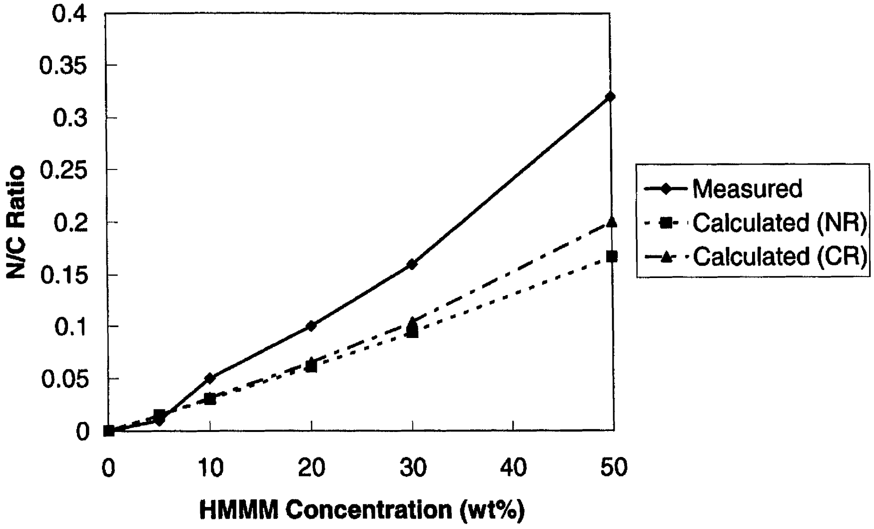

FIGURE 6 Surface N/C ratio for HMMM/polyesters, as a function of HMMM concentration.

components only) and complete reaction (CR) of the HMMM methoxy moieties, as a function of HMMM content. The figure shows that at all compositions above 5 wt% HMMM the nitrogen content in the surface is greater than that predicted from bulk composition calculations, which is indicative of melamine enrichment at the surface.

The second method uses atomic concentrations derived from deconvoluted C_{ls} spectra and is based on the premise that C-N species derive only from melamine, and C=O species derive only from polyester. Thus, the ratio $\underline{C}$–N/$\underline{C}$=O, depending on the deconvolution accuracy, should indicate directly the ratio of melamine to polyester at the surface. This ratio is shown in Figure 7 as a function of HMMM concentration, which also compares the experimental value with that which would be expected from bulk composition calculations. The figure shows that at or below 20 wt% HMMM the surface melamine content is identical to or very slightly lower than that which would be expected in the bulk. However, above 20 wt% the melamine content of the surface is increased, and above 30 wt% HMMM it is considerably increased, compared with the expected bulk composition.

Although both XPS analysis methods have limitations, both methods give essentially the same conclusions in this study. The results from survey spectra can be complicated by interference from adsorbed atmospheric nitrogen and adventitious carbon, and thus

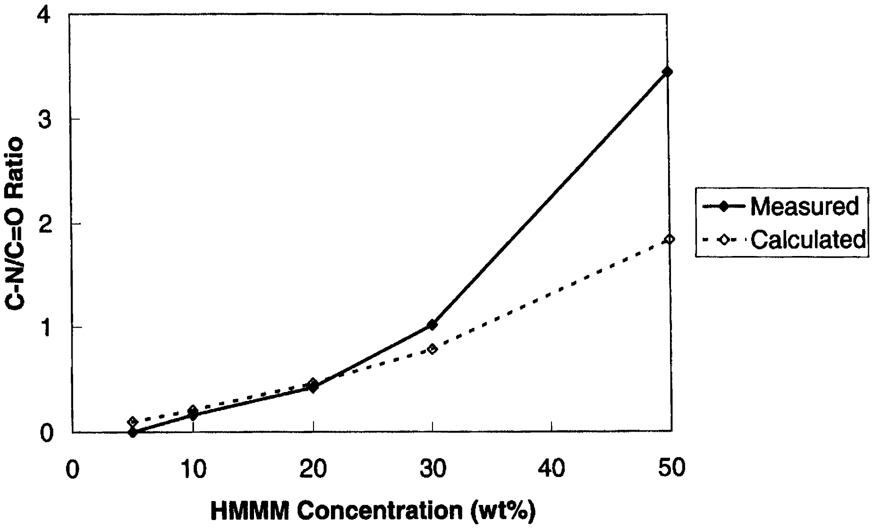

FIGURE 7 Surface $\underline{C}$–N/$\underline{C}$=O ratio for HMMM/polyesters, as a function of HMMM concentration.

may not be quantitative. On the other hand, the deconvolution method is a mathematical construct that involves a number of assumptions about the possible surface chemistries. In the present case, the results of the two methods are qualitatively similar, showing nitrogen-containing species at greater concentrations than expected from bulk composition when the melamine content is high.

These results are also consistent with those published recently [2] using HMMM/polyester films detached from the substrate. In that study, the coating/substrate interface was also studied, and it was found that melamine was depleted at the substrate interface. Thermal characterisation of HMMM/polyester coatings prepared under rapid-cure (nonisothermal) conditions [1] showed that at high melamine concentrations there was evidence from dynamic mechanical analysis (DMA) measurements of two partially phase-separated networks: a cocondensed polyester-melamine network and a self-condensed melamine–melamine network. On the basis of surface analysis results (this work and Gamage *et al.* [2]), it can be concluded that the second, self-condensed melamine network that is formed under rapid-cure conditions tends to be concentrated in the upper layers of the coating towards the air/coating interface.

Of relevance to the interpretation of the adhesion results in Figure 2 is the observation made by Gamage *et al.* [1] that the self-condensed network has a higher Tg than the cocondensed polyester–melamine network. The Tg of the melamine network has been shown by DMA [1] to increase from ~30°C at low HMMM content up to ~70°C at the highest concentration used (50 wt%). Thus, as the HMMM content is increased, the surface becomes increasingly glassy, due to the concentration at the surface of the self-condensed HMMM network. The XPS results show that above a certain composition (~20 wt%) the particle would be expected to interact with the melamine–melamine network at the surface. The glassy nature of the network would lead to lower adhesion, as observed. The lower adhesion comes from reduced contact because of the less-deformable asperities and from a reduced energy dissipation in the highly crosslinked network.

CONCLUSIONS

Particle adhesion to polyester-melamine clearcoats containing low concentrations (<20 wt%) of HMMM displays behaviour reminiscent of pressure-sensitive adhesives. That is, as the temperature is increased the adhesion reaches a maximum at slightly above the bulk Tg and then decreases with further increase in temperature. Above a critical concentration of HMMM, however, particle adhesion is dramatically reduced at all temperatures studied, both above and below the bulk Tg. The reason for the decrease in adhesion is not believed to be connected with the bulk Tg or surface energy, both of which did not vary greatly with melamine content. The generation of a segregated melamine–melamine network at the surface of high-HMMM formulations is believed to be the primary cause of the low particle adhesion. A small excess of HMMM crosslinker promotes the formation of a self-condensed melamine–melamine network, and XPS evidence suggests that this network is concentrated at the surface rather than homogeneously distributed throughout the coating. Thus the particle interacts with an increasingly glassy surface as the crosslinker concentration increases, and it is well-known that adhesion to polymers below Tg is typically low since it is largely associated with asperity contact only.

The results presented here suggest that a small addition of excess HMMM to an otherwise optimized polyester–melamine formulation could lead to a dramatic change in the particle adhesion behaviour. It is unlikely that small changes in melamine content would seriously compromise other desirable properties, such as appearance and flexibility.

REFERENCES

[1] Gamage, N. J. W., Hill, D. J. T., Lukey, C. A., and Pomery, P. J., *J. Poly. Sci.: Poly. Chem. Ed.* **41**, 1603–1621 (2003).

[2] Gamage, N. J. W., Hill, D. J. T., Lukey, C. A., and Pomery, P. J., *J. Poly. Sci.: Poly. Chem. Ed.*, **42**, 83–91 (2004).

[3] Dupré, A., *Theorie Mechanique de La Chaleur*, (Gauthier-Villars, Paris, 1869).

[4] Kendall, K., *Science* **263**, 1720–1725 (1994).

[5] Toikka, G., Spinks, G. M., and Brown, H. R., *J. Adhes.* **74**, 317–340 (2000).

[6] Toikka, G., Spinks, G. M., and Brown, H. R., *Langmuir* **17**, 6207–6212 (2001).

[7] Johnson, K. L., Kendall, K., and Roberts, A. D., *Proc. Roy. Soc. London* **A324**, 301–313 (1971).

[8] Kobayashi, H. and Owen, M. J., *Macromolecules* **23**, 4929–4933 (1990).

[9] Clint, J. H. and Wicks, A. C., *Int. J. Adhes. Adhesives* **21**, 267–273 (2001).

[10] Taru, Y. and Takaoka, K., *J. Japan Soc. Col. Mat.* **58**, 661–667 (1985).

[11] Beamson, G. and Briggs, D., *High Resolution XPS of Polymers—The Scienta ASCA300 Database* (John Wiley & Sons, New York, 1992).

[12] Leadley, S. R., Watts, J. F., Blomfield, C. J., and Lowe, C., *Surf. Interface Anal.* **26**, 444–454 (1998).